2013

Loess origin, transport, and deposition over the past 10,000 years, Wrangell-St. Elias National Park, Alaska

Daniel R. Muhs
U.S. Geological Survey, dmuhs@usgs.gov

James R. Budahn
US Geological Survey

John P. McGeehin
U.S. Geological Survey

E. Arthur Bettis III
University of Iowa, art-bettis@uiowa.edu

Gary Skipp
U.S. Geological Survey, gskipp@usgs.gov

See next page for additional authors

Authors
Daniel R. Muhs, James R. Budahn, John P. McGeehin, E. Arthur Bettis III, Gary Skipp, James B. Paces, and Elisabeth A. Wheeler

Aeolian Research 11 (2013) 85–99

Contents lists available at SciVerse ScienceDirect

Aeolian Research

journal homepage: www.elsevier.com/locate/aeolia

Loess origin, transport, and deposition over the past 10,000 years, Wrangell-St. Elias National Park, Alaska

Daniel R. Muhs [a,*], James R. Budahn [a], John P. McGeehin [b], E. Arthur Bettis III [c], Gary Skipp [a], James B. Paces [a], Elisabeth A. Wheeler [d]

[a] U.S. Geological Survey, MS 980, Box 25046, Federal Center, Denver, CO 80225, United States
[b] U.S. Geological Survey, MS 926A, National Center, Reston, VA 20192, United States
[c] Department of Geoscience, University of Iowa, Iowa City, IA 52242, United States
[d] Department of Forest Biomaterials, North Carolina State University, 2105 Biltmore Hall, Raleigh, NC 27695, United States

ARTICLE INFO

Article history:
Received 2 April 2013
Revised 4 June 2013
Accepted 5 June 2013
Available online 10 July 2013

Keywords:
Loess
Dust
Holocene
Last glacial period
Wrangell-St. Elias National Park, Alaska
Radiocarbon dating

ABSTRACT

Contemporary glaciogenic dust has not received much attention, because most research has been on glaciogenic dust of the last glacial period or non-glaciogenic dust of the present interglacial period. Nevertheless, dust from modern glaciogenic sources may be important for Fe inputs to primary producers in the ocean. Adjacent to the subarctic Pacific Ocean, we studied a loess section near Chitina, Alaska along the Copper River in Wrangell-St. Elias National Park, where dust has been accumulating over the past ~10,000 years. Mass accumulation rates for the fine-grained (<20 μm) fraction of this loess section are among the highest reported for the Holocene of high-latitude regions of the Northern Hemisphere. Based on mineralogy and geochemistry, loess at Chitina is derived from glacial sources in the Wrangell Mountains, the Chugach Mountains, and probably the Alaska Range. Concentrations of Fe in the silt-plus-clay fraction of the loess at Chitina are much higher than in all other loess bodies in North America and higher than most loess bodies on other continents. The very fine-grained (<2 μm) portion of this sediment, capable of long-range transport, is dominated by Fe-rich chlorite, which can yield Fe readily to primary producers in the ocean. Examination of satellite imagery shows that dust from the Copper River is transported by wind on a regular basis to the North Pacific Ocean. This Alaskan example shows that high-latitude glaciogenic dust needs to be considered as a significant Fe source to primary producers in the open ocean.

Published by Elsevier B.V.

1. Introduction

Dust is an integral part of the Earth's environmental systems, including the atmosphere, geosphere, hydrosphere, and biosphere. A number of reviews in the past decade or so have emphasized the importance of dust with its influence on planetary radiation balance, effects on clouds and precipitation, its role in adding nutrients to soils and the biosphere, and the importance of dust as a source of iron to primary producers (such as phytoplankton) in the world's oceans (Kohfeld and Harrison, 2001; Tegen, 2003; Goudie and Middleton, 2006; Mahowald et al., 2005, 2006; Kohfeld and Tegen, 2007; Maher et al., 2010; Shao et al., 2011; Muhs, 2013a). These reviews also show that the emphasis of dust research has been on either contemporary dust sources, dominantly in low-latitude arid regions, or enhanced dust production at higher latitudes during the last glacial period. There has been a focus on contemporary dust sources at low latitudes because satellite-based global studies show that such regions are unquestionably the most important dust sources at the present time (Prospero et al., 2002). Concentration of studies on mid-latitude and high-latitude dust sources during the last glacial period is also understandable, because dust production globally during this time was much greater than at present, as seen in ice core records (EPICA Community Members, 2004; Ruth et al., 2007), deep-sea core records (Rea, 1994, 2007), and loess records (Muhs, 2013b).

In contrast, there has been little study of modern, high-latitude dust sources, which come primarily from glacial sources. Bullard (2012), who recently reviewed this topic in detail, points out that (1) high-latitude, glaciogenic dust sources have been underemphasized or even ignored by many aeolian researchers; (2) there are limited quantitative data on the contributions of contemporary glaciogenic dust to the overall dust cycle, particularly over long timescales; (3) where dust flux rates in such environments have been measured, they are sometimes very high; and (4) the significance of high-latitude glaciogenic dust likely will increase over time with global warming, as mountain glaciers and ice sheets ablate and dust supplies increase. Potential glaciogenic dust sources

* Corresponding author. Fax: +1 303 236 5349.
E-mail address: dmuhs@usgs.gov (D.R. Muhs).

1875-9637/$ - see front matter Published by Elsevier B.V.
http://dx.doi.org/10.1016/j.aeolia.2013.06.001

exist over a wide span of the circum-Arctic region, including Greenland, Iceland, Svalbard, northern Russian islands (Zemlya Frantsa Iosifa, Novaya Zemlya, Severnaya Zemlya), the Queen Elizabeth Islands and Baffin Island of Canada, the mountains of western Canada, and southern Alaska (Fig. 1). Arnalds (2010) and Prospero et al. (2012) provide examples of the importance of contemporary glaciogenic dust inputs to the North Atlantic Ocean from Iceland. Silt-and-clay-rich soils derived from this dust cover a significant portion of Iceland (Arnalds, 2004), with dust deposition rates ranging up to 500 g/m^2/yr (Arnalds, 2010). Jackson et al. (2005) show that dust deposition as loess has been an ongoing process in Iceland for at least 10,000 years.

In parallel to the studies of Arnalds (2010) and Prospero et al. (2012) for the North Atlantic Ocean, we wished to determine the potential significance of contemporary, high-latitude dust inputs to the North Pacific Ocean. Southern Alaska, where glaciers are widespread, borders the North Pacific Ocean (Fig. 1), and much of Alaska, including the southern part of the state, is mantled with loess (Fig. 2). A review of many of the localities where loess stratigraphic studies have been conducted shows that the uppermost loess over much of Alaska is of Holocene age (Muhs et al., 2003), indicating that dust production has been a widespread process in the present interglacial period. Recent studies by Crusius et al. (2011) and Bullard (2012) show that dust inputs to the North Pacific Ocean from glaciated southern Alaska, specifically, the Copper River basin, are significant at present. Further, Boyd et al. (1998), Schroth et al. (2009), and Crusius et al. (2011) have emphasized the potential importance of dust inputs from southern Alaska to the North Pacific Ocean as a source of Fe for phytoplankton. The North Pacific Ocean, specifically the subarctic eastern Pacific Ocean, has been recognized as one of three regions in the world (the eastern equatorial Pacific Ocean and the Southern Ocean are the other two) where there are Fe limitations to primary production (Boyd et al., 1998; Falkowski et al., 1998; Lam and Bishop, 2008).

In order to understand contemporary loess genesis in a high-latitude region and assess the significance of dust inputs to the North Pacific Ocean, we sought a long-term, geologic record of dust deposition in southern Alaska. Loess deposits have been recognized in the Copper River basin of Alaska for at least a century. Tarr and Martin (1913) describe thick loess deposits adjacent to the Copper River that contain buried tree stumps, indicating the potential for developing a chronology for dust deposition. We found a loess section near Chitina, Alaska that we believe is very close to those described by Tarr and Martin (1913), Rubin and Alexander (1960), and Ager (1989). The goals in studying this loess section were to: (1) determine the duration, in recent geologic time, over which dust inputs to the North Pacific Ocean from aeolian sources may have been important by using a nearby terrestrial record; (2) determine the source of this loess, using mineralogy and geochemistry; (3) ascertain what the Fe content is in the fine-grained fraction of loess, specifically those particles that are capable of longer-range transport to the ocean; and (4) characterize the mineralogy of the fine-grained portion of the loess, in order to assess whether Fe in that size fraction is potentially bioavailable in seawater.

2. Geologic history of the study area

The Copper River basin is surrounded by the Wrangell Mountains, Chugach Mountains, Talkeetna Mountains, and the Alaska Range (Fig. 3). The Chitina loess section is close to the Copper River and is situated within Wrangell-St. Elias National Park, an area that is complex geologically (Plafker et al., 1989; Winkler et al., 2000; Richter et al., 2006). Mountain building by exotic terrane accretion

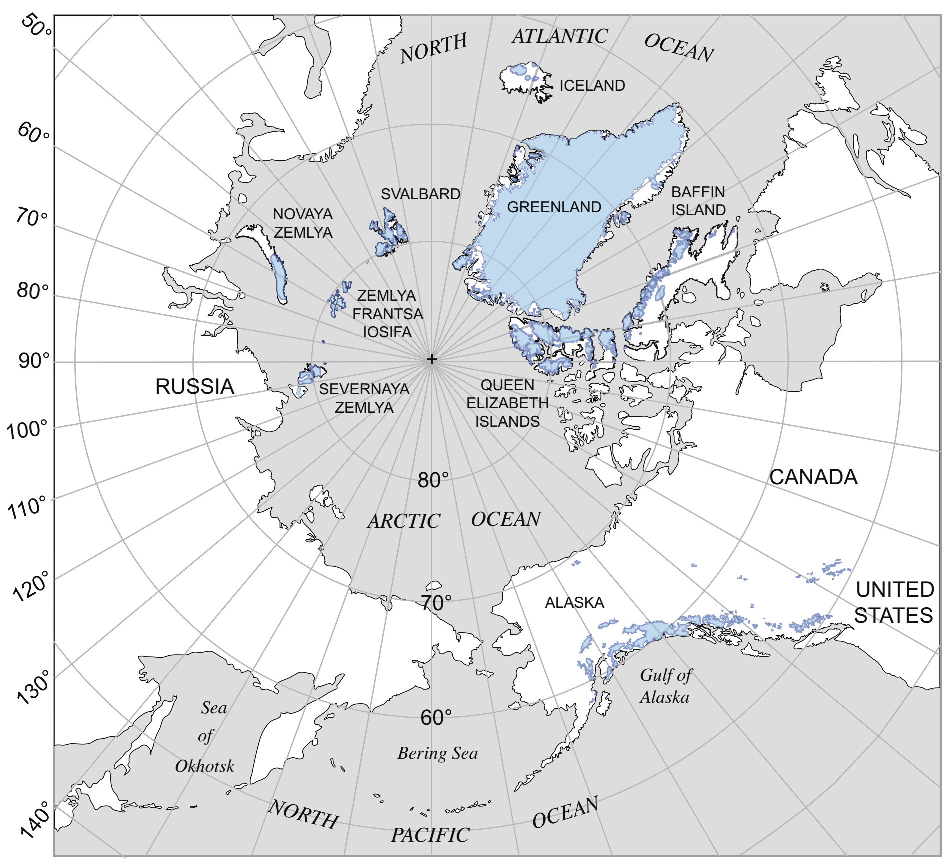

Fig. 1. Map of the circum-Arctic region, showing distribution of contemporary glaciers, ice caps, and ice sheets (blue) that are potential sources of glaciogenic dust. Redrawn in simplified form from Brown et al. (1997). (For interpretation of the references to colour in this figure legend, the reader is referred to the web version of this article.)

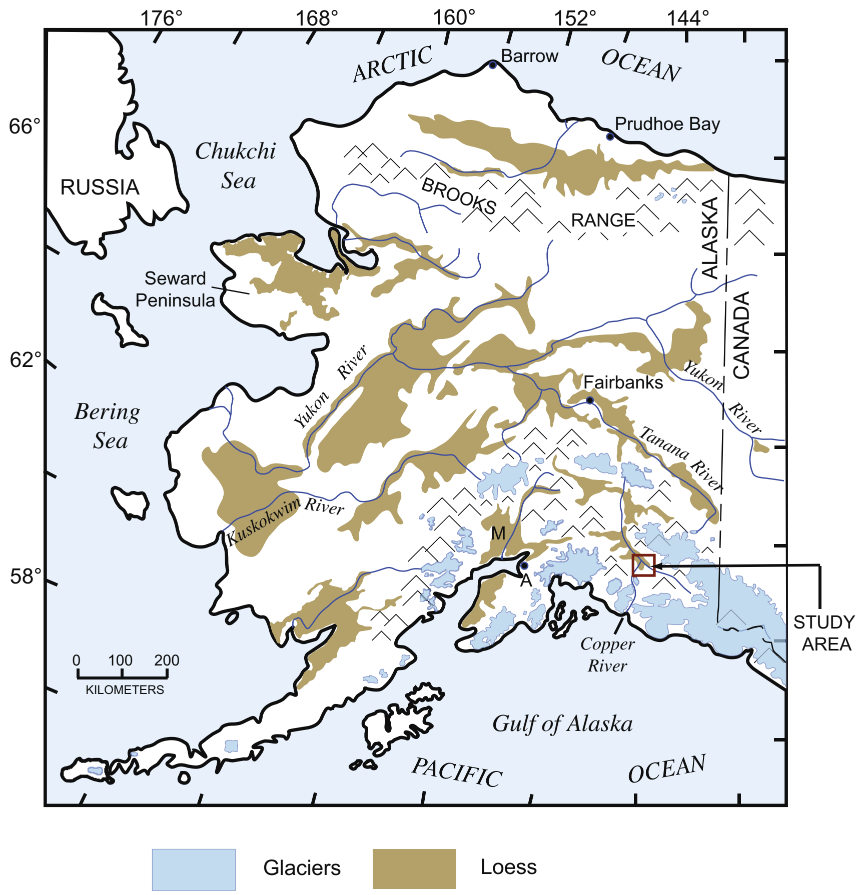

Fig. 2. Map showing the distribution of loess deposits (brown) in Alaska, compiled from Hopkins (1963) and Sainsbury (1972) for the Seward Peninsula and Péwé (1975) for all other parts of the region. Most mapping from these sources has been field checked by the authors. Also shown is the present extent of glaciers (blue) in the region, taken from Péwé (1975) and Brown et al. (1997). A, Anchorage; M, Matanuska valley. (For interpretation of the references to colour in this figure legend, the reader is referred to the web version of this article.)

from plate movement, volcanism, and movement along faults has created spectacular, rugged peaks in the Wrangell Mountains. As a result, glaciers are extensive in the Wrangell Mountains at present and were more extensive during the last glacial period, as is the case with the nearby Chugach Mountains, Alaska Range, and Talkeetna Mountains (Fig. 3).

Loess at Chitina was likely derived from glaciogenic silts entrained by wind from the Copper River floodplain (Fig. 4). At times in the past, however, this river floodplain was not available as a dust source. During periods when glacial ice advanced far enough down valleys of mountain ranges surrounding the basin, drainage of the north-to-south-flowing Copper River was blocked and large lakes formed (Nichols, 1989; Williams, 1989; Ferrians, 1989; Wiedmer et al., 2010). The most recent glacier-dammed lake that formed in the Copper River basin has been called Glacial Lake Atna (Fig. 3). Radiocarbon ages suggest that Glacial Lake Atna formed sometime before ~38,000 ^{14}C yr BP, perhaps reached its highest elevation ~18,000 ^{14}C yr BP and was gone by ~9400 ^{14}C yr BP (Ferrians, 1989; Williams, 1989). While Glacial Lake Atna was extant, source sediments for loess would be submerged. Thus, a prerequisite for loess accumulation was drainage of the lake due to ice recession, at the start of the Holocene.

3. Methods

Radiocarbon dating of wood and other plant fragments found in the section at Chitina was done by accelerator mass spectrometry (AMS) following McGeehin et al. (2001). AMS radiocarbon measurements were made at the Center for Accelerator Mass Spectrometry (CAMS) at Lawrence Livermore National Laboratory. Calibrated ages (Table 1), designated as calibrated years before present (cal yr BP), were derived using the OxCal 4.1 calibration software (Bronk Ramsey, 2009) in conjunction with the IntCal09 calibration curve (Reimer et al., 2009). For loess particle size distribution, pretreatments included destruction of organic matter with hydrogen peroxide, removal of carbonates with acetic acid, and dispersion with sodium hexametaphosphate. Sand (2 mm to 53 μm), coarse silt (53–20 μm), fine silt (20–2 μm), and clay (<2 μm) contents were determined by wet-seiving, settling, and pipette. Abundances of these size fractions are reported as weight-percents. Bulk mineralogy on whole-sediment and silt-plus-clay fractions was determined by X-ray diffractometry (XRD). Sediments from selected depths were also analyzed for clay (<2 μm) mineralogy, also by XRD. For these analyses, clays were separated by sedimentation after removal of organic material with hydrogen peroxide, removal of carbonates with buffered acetic acid, and dispersion with sodium hexametaphosphate. Clay samples were X-rayed three times: in an air-dry state, after glycolation, and after heat treatment (550 °C for 1 h). Clay mineral identification follows Moore and Reynolds (1989). Organic carbon and carbonate mineral (calcite and dolomite) contents were measured by coulometric titration, following Engleman et al. (1985).

Concentrations (weight percents or ppm) of selected major and trace elements were determined by energy-dispersive X-ray fluorescence (ED XRF) on pulverized bulk samples. The silt-plus-clay fraction (<53 μm) was extracted from bulk samples by wet-sieving,

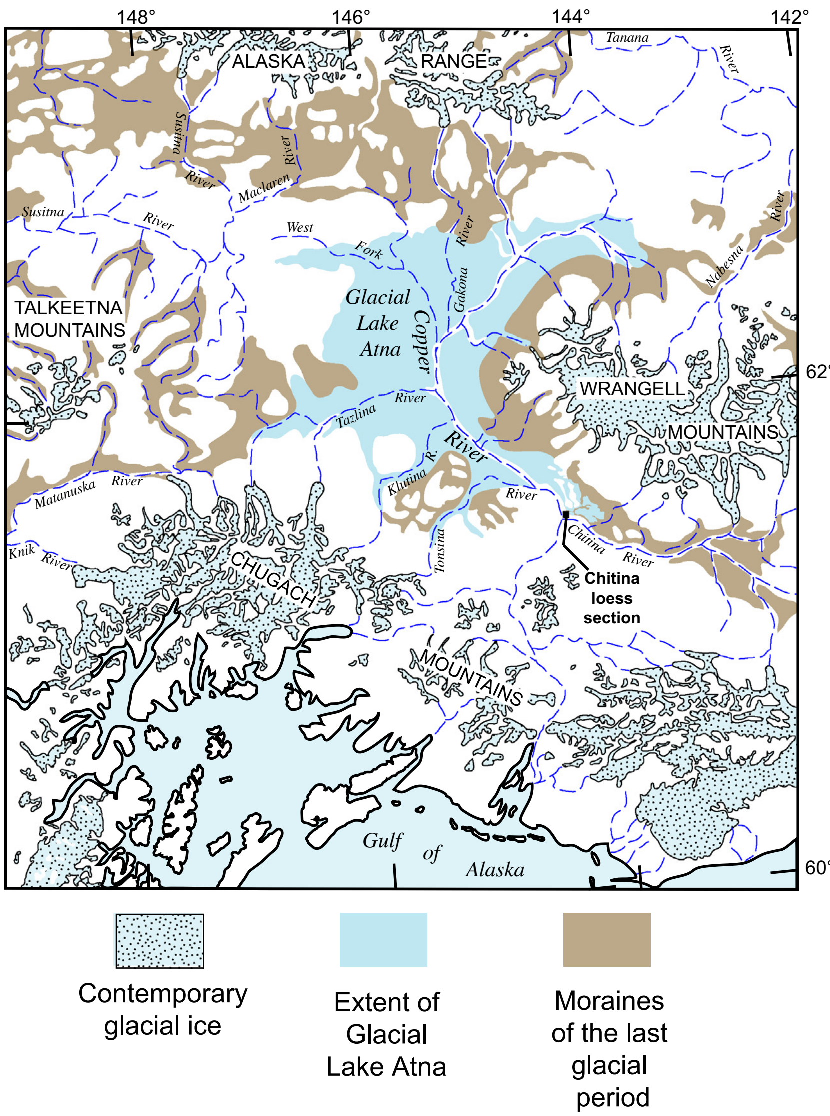

Fig. 3. Map showing the Copper River basin, surrounding mountain ranges, extent of present glaciers (light blue and stippled), moraines of last-glacial age (brown), extent of Glacial Lake Atna (blue), and location of the loess section studied near Chitina. Moraines taken from Karlstrom et al. (1964); Glacial Lake Atna from Williams (1989). (For interpretation of the references to colour in this figure legend, the reader is referred to the web version of this article.)

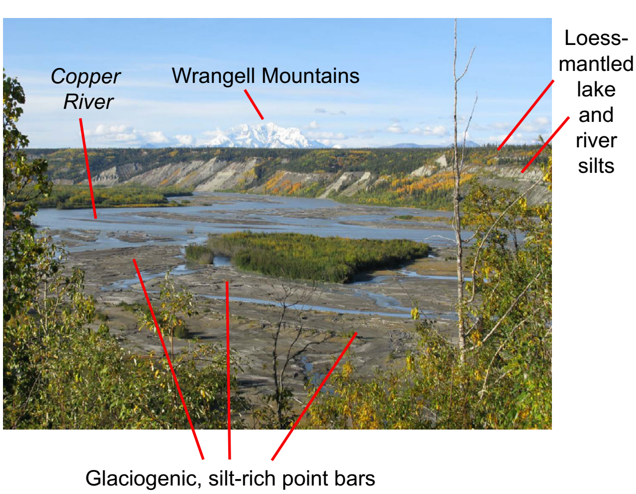

Fig. 4. View of part of the Wrangell Mountains, the Copper River (with silt-rich point bars), and river valley sides mantled by Glacial Lake Atna sediments, aeolian sand, and loess.

after destruction of organic matter with H_2O_2 and dispersion with sodium pyrophosphate (but without removal of carbonates). This fraction was analyzed for all major elements by wavelength-dispersive X-ray fluorescence (WD XRF). The <53 μm fraction was also analyzed by instrumental neutron activation analysis (INAA) for trace elements following Budahn and Wandless (2002).

4. Stratigraphy, sedimentology, radiocarbon ages, and mass accumulation rates

The road cut near Chitina exposes more than 10 m of Quaternary sediments (Fig. 5). The base of the exposure exhibits a gravel-rich diamicton that we interpret to be till dating to the last (Wisconsin) glacial period. Richter et al. (2006) map glacial drift on both sides of the Chitina River upstream of our study locality that they correlated to the Wisconsin glacial period. Ice that deposited these sediments originated from several valley glaciers on the southwestern side of the Wrangell Mountains (Fig. 3).

Almost 9.5 m of aeolian deposits cover the glacial gravels at Chitina (Figs. 5 and 6). The lower ~1 m of aeolian sediments, immedi-

Table 1
Wood identifications, sample depths, radiocarbon ages and calibrated ages for the Chitina loess section.

Field #	USGS lab #	CAMS #	Depth (cm)	Material	δ^{13}C (o/oo)	Age (yr BP)	Error (yr; 1 sigma)	2-sigma Calibrated age (cal yr BP		
								From	To	Median
AK-1704A	WW7766	146777	75–100	Probable *Picea*	-26.7	1000	30	969	797	883
AK-1705A	WW7767	146778	100–125	Probable *Picea*	-25.6	1480	35	1484	1300	1392
AK-1706A	WW7768	146779	125–150	Probable *Picea*	-28.4	1450	25	1385	1301	1343
AK-1707A	WW7769	146780	150–175	*Picea*	-26.6	1770	30	1813	1605	1709
AK-1709A	WW7770	146781	200–225	Cupressaceae?	-24.4	2095	25	2140	1996	2068
AK-1710A	WW7771	146782	225–250	Conifer wood	-25.4	2195	25	2315	2140	2228
AK-1711A	WW7772	146783	250–275	*Picea* or *Larix*	-25.5	2205	25	2316	2149	2232
AK-1714A	WW7773	146784	325–350	Probable *Picea*	-25.2	3075	30	3365	3216	3290
AK-1715A	WW7774	146785	350–375	*Picea*	-26.3	3345	25	3679	3481	3580
AK-1716A	WW7775	146786	375–400	*Picea*	-25.4	3440	30	3829	3631	3730
AK-1717A	WW7776	146787	400–425	Probable *Picea*	-25.2	3385	25	3692	3572	3632
AK-1719A	WW7777	146788	450–475	Probable *Picea*	-25.2	4045	25	4780	4429	4604
AK-1721A	WW7778	146790	500–525	Pinaceae	-29.3	4425	25	5263	4874	5068
AK-1722A	WW7779	146791	525–550	*Picea*	-25.7	4510	25	5299	5050	5174
AK-1723A	WW7780	146792	550–575	*Picea*	-26.1	4765	30	5589	5333	5461
AK-1725A	WW7781	146793	600–625	Probable *Picea*	-26.1	5275	35	6182	5940	6061
AK-1726A	WW7782	146794	625–650	*Picea*	-25.5	5370	30	6279	6015	6147
AK-1727A	WW7783	146795	650–675	Probable conifer	-27.2	5845	30	6740	6564	6652
AK-1730A	WW7784	146796	725–750	*Picea*	-26.8	6965	30	7921	7701	7811
AK-1731A	WW8342	151127	750–775	Pinaceae	-26.0	7885	25	8774	8595	8684
AK-1732A	WW8343	151128	775–800	Probable *Picea*	-24.3	8150	25	9240	9011	9126
AK-1734A	WW8344	151129	800–813	Plant fragments	-25.0	8135	25	9128	9009	9068
AK-1735	WW8390	151253	813–820	Plant fragments	-27.6	8145	40	9252	9005	9129
AK-1738A	WW8348	151130	865–888	Plant fragments	-27.4	9100	25	10277	10208	10242

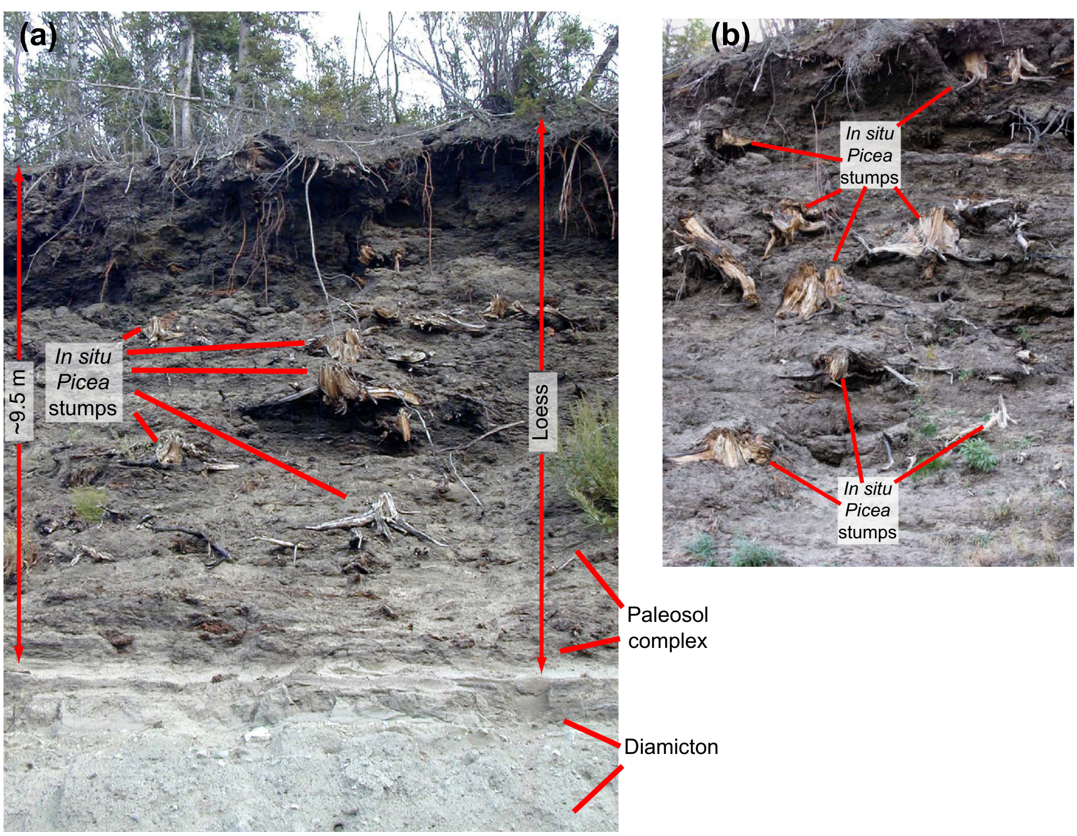

Fig. 5. Photographs of the Chitina loess section, showing (a) aeolian sediments, growth-position tree stumps and underlying diamicton; and (b) close-up of in situ *Picea* (spruce) stumps.

ately above the glacial gravels, is a series of sand-rich (~30–60% sand) beds intercalated with minimally developed paleosols. The paleosols indicate that aeolian deposition during this interval was episodic. We also found as many as 3 tephras, identified as thin, white bands that contrast strongly with brown loess within this zone. From ~8 m depth to the surface, however, the section is characterized by crudely laminated loess that is richer in silt and clay. Total silt (53–2 μm) content ranges from 50% to 70%

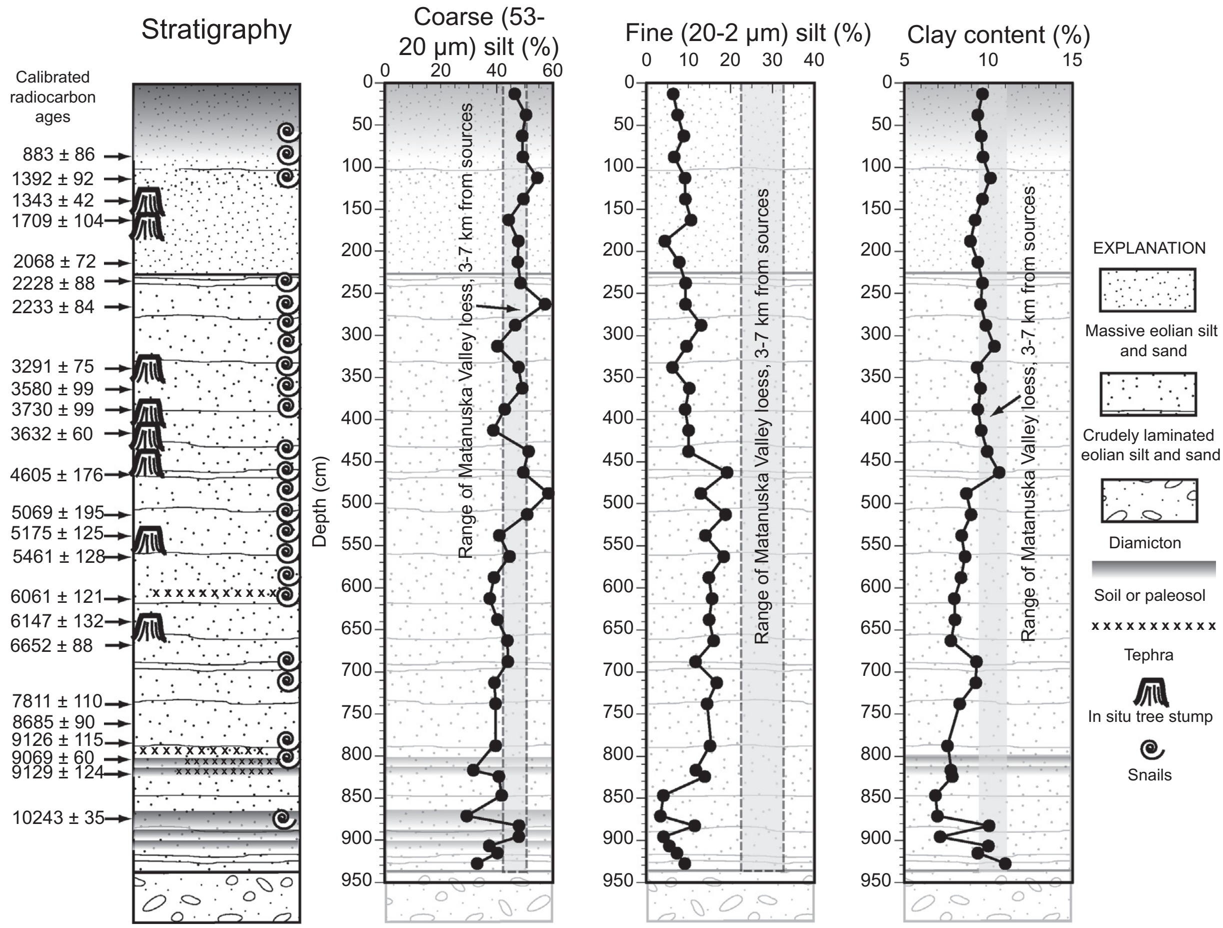

Fig. 6. Stratigraphy, radiocarbon ages, and coarse silt, fine silt, and clay contents in the Chitina loess section. Shown for comparison (gray bands) are the ranges of silt and clay in loess ~3 to ~7 km away from sources in the Matanuska River valley, southern Alaska (Matanuska data from Muhs et al., 2004).

and total silt-plus-clay in the upper ~8 m ranges from 59–80%. Within the silt fraction, coarse silt (53–20 μm) ranges from 38% to 58% and fine silt (20–2 μm) ranges from 4% to 19% (Fig. 6). Clay (<2 μm) content shows little variation throughout the section and ranges from 7% to 11%. Overall, the particle size distribution is similar to, or slightly coarser than loess in the Matanuska Valley of southern Alaska (Fig. 2) where it is found ~3 to 7 km from its probable sources (Muhs et al., 2004). This is consistent with an interpretation that the nearby Copper River and its tributaries were the immediate sources of aeolian sediment at Chitina.

Paleosols are not apparent from ~8 m depth up to the modern soil, indicating that deposition was not interrupted by long periods of no sedimentation. Nevertheless, aeolian sedimentation did not take place in the absence of a vegetation cover. Aeolian deposition apparently occurred contemporaneously with boreal forest growth. Organic carbon content is relatively high (4–11%; average, 7%) throughout the section above ~8 m, and land snails (Succineidae) are present, suggesting aeolian accretion on a vegetated surface. The most definitive evidence of aeolian deposition on vegetated surfaces is the presence of remarkably well-preserved tree stumps, including 8 of these features at depths of ~1.5–6.5 m, similar to those reported by Tarr and Martin (1913). Even where stumps are not preserved in the section, wood fragments are found throughout, to a depth of ~8.7 m.

AMS radiocarbon ages were determined on 24 specimens of wood or other plant materials (Table 1). Dating of these materials yields a stratigraphically consistent suite of ages through the main part of the aeolian section. Of the wood fragments, seven could be clearly identified as *Picea*, with an additional eight specimens that are likely *Picea*. A probable *Picea* specimen found at a depth of 7.75–8.0 m has a radiocarbon age of 8150 ± 25 ^{14}C yr BP (~9100 cal yr BP). *Picea*, therefore, probably has been in the southern Copper River basin for at least the past ~9100 cal yr, similar to what has been reported from a sediment core record at Grizzly Lake, ~130 km to the north of Chitina (Tinner et al., 2006). There are *apparent* slight age reversals in three zones (1.0–1.5 m; 3.75–4.25 m; 7.75–8.13 m) between three adjacent pairs of samples. However, the ages of adjacent pairs are actually in agreement with each other within limits of analytical uncertainty, both with uncalibrated radiocarbon ages and with calibrated ages (at 2-sigma). Overall, we regard the chronology as robust. Our lowermost sample, at a depth of 8.65–8.88 m, is plant material within the uppermost of three paleosols, and gives an age of 9100 ± 25 ^{14}C yr BP (~10,200 cal yr BP). We interpret this as a reasonable minimum-limiting age for the glacial gravels, and it supports correlation of the underlying glacial deposits with the late Wisconsin advance of ice out of the Wrangell Mountains. Thus, dust transport from the Copper River floodplain has been an ongoing process for the past ~10,000 years.

In order to compare dust flux rates in different geologic archives (loess, deep-sea cores, lake cores, ice cores), it is useful to compute mass accumulation rates (MARs). Typically, MARs are expressed in units of g/m^2/yr. In a loess section such as that at Chitina, we can estimate dust MARs by knowing the vertical sedimentation rate (cm/yr), the bulk density (g/cm^3), the fraction of sediment that is mineral matter (computed by subtracting organic matter content), and the fraction of the mineral matter that is capable of long-range transport (<20 μm). The upper 800 cm of the section, where we have the best age control, was deposited in the past ~9000 cal yr, yielding an average vertical sedimentation rate of 0.09 cm/yr. We did not measure bulk density at Chitina, but we can use a range of values that have been reported for loess and loess-derived soils found elsewhere in Alaska. Muhs et al. (2003) report that unaltered loess in central Alaska has bulk density values of 1.2–1.5 g/cm^3. Soil A horizons with more organic matter have bulk density values somewhat lower than this but still greater than 1.0 g/cm^3, and soil O horizons typically have values significantly lower than 1.0 g/cm^3. Here, in order to span the range of possible bulk densities at Chitina, we computed MARs using bulk density values of 0.5, 1.0, and 1.5 g/cm^3. Organic carbon content in these sediments, as discussed above, ranges from 4% to 11%, with a mean value of 7%, which we use in our calculations. Organic matter content can be estimated by multiplying organic carbon content by 1.724 (Birkeland, 1999), yielding an average organic matter content of 12% and a mineral matter content of 88%. Particle size analyses indicate that the average sum of fine silt (20–2 μm) and clay (<2 μm) in the section at Chitina is 20–21%. Thus, assuming a bulk density of 1.0 g/cm^3, there is 0.88 g/cm^3 of mineral matter and of this, 0.176 g/cm^3 of fine grained (<20 μm) particles. Using the sedimentation rate computed above (0.09 cm/yr), this yields a MAR of 0.0158 g/cm^2/yr, or 158 g/m^2/yr. If we assume a lower bulk density of 0.5 g/cm^3, the rate is 78 g/m^2/yr; assumption of a typical loess bulk density of 1.5 g/cm^3 yields a rate of 237 g/m^2/yr. Given the organic matter contents we measured at Chitina, we suspect that the lower range of values, 78–158 g/m^2/yr, is probably more accurate.

5. Mineralogy and geochemistry

5.1. Bulk mineralogy and major element geochemistry

The silicate minerals in bulk samples from Chitina (all size fractions) are quartz, plagioclase, K-feldspar, amphibole, and chlorite, found at all depths. Mica and carbonate minerals (calcite and dolomite) are also found at most depths. Total carbonate contents range from 0 (upper part of the section) to 15% (lower part), with values of 2–10% in most of the middle part of the section. The presence of carbonates in loess at Chitina differs from other southern Alaskan loess deposits. Matanuska Valley loess (Fig. 2) lacks both calcite and dolomite (Fig. 7a).

Major element geochemistry, done by ED XRF on bulk samples, is consistent with the mineralogy of quartz, plagioclase, K-feldspar, amphibole, chlorite, mica, calcite and dolomite. Total Fe contents (as Fe_2O_3) range from 5.8% to 6.8% and probably reflect the relatively high abundance of chlorite and amphibole. Moderate amounts of K-feldspar and mica are consistent with K_2O contents that range from 1.4% to 2.1%. The presence of the carbonate minerals, calcite and dolomite, is reflected in CaO contents that range from 7% to 7% and Sr contents that range from ~340 to ~420 ppm (Fig. 7b).

5.2. Silt +clay mineralogy and major element geochemistry

Because our primary goal is to understand the fine-grained (dust) component of the Chitina section that is capable of long-distance transport, we analyzed the mineralogy of the silt-plus-clay (<53 μm) fraction separately and also conducted major element geochemical analyses of this fraction. Quartz, plagioclase, amphibole and chlorite are present in the < 53 μm fraction at all depths in the section, and dolomite and/or calcite were detected in all but a few samples. K-feldspar is in two-thirds of the samples and mica is in a third of the samples. Overall, the mineralogy of the <53 μm fraction is very similar to the bulk mineralogy. Within this silt + clay fraction, concentrations of SiO_2 range from ~50% to 62%, with most values ~55–59%, and Al_2O_3 concentrations show a narrow range of 12–14%. The presence of chlorite and amphibole is reflected in the Fe_2O_3 content, which ranges from 6.3% to 7.3%. Carbonates (calcite and dolomite) are expressed in CaO concentrations that range from 6% to 12% and loss-on-ignition (LOI) values that range from 3% to 10%. Plagioclase and amphibole are represented by Na_2O, which ranges from 2.6% to 3.2% and K-feldspar and mica are represented by K_2O, which ranges from 1.2% to 1.5%.

5.3. Clay mineralogy

Clay mineral analyses indicate that chlorite, smectite, and mica are the dominant minerals in the clay fraction of all samples, with much smaller amounts of quartz, plagioclase and possibly kaolinite (Fig. 8). Chlorite is the most abundant of the clay minerals, based on peak heights. Based on the higher (002) and (004) peaks compared to the (001) and (003) peaks, this chlorite is Fe-rich. Smaller amounts of mica are found in all samples, and most samples also contain smectite. Based on the decrease in the heights of the

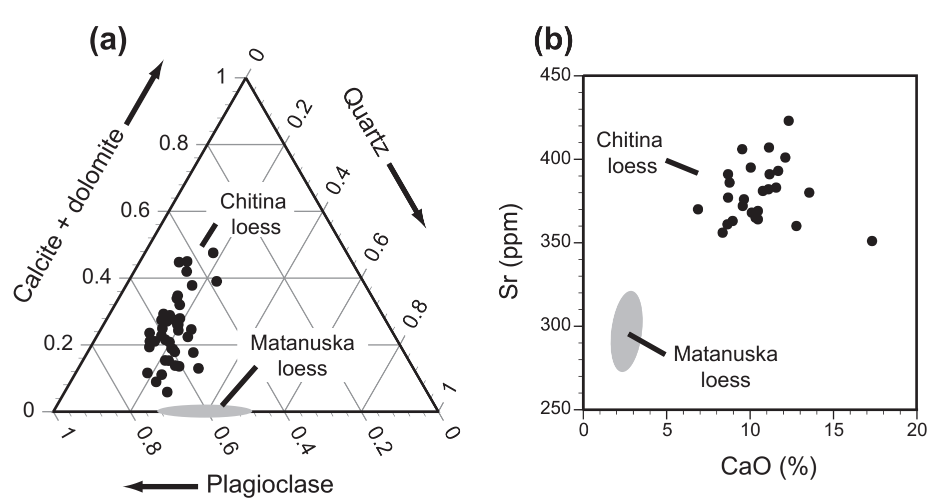

Fig. 7. (a) Ternary diagram of bulk mineralogy at Chitina, compared to Holocene loess from the Matanuska Valley, southern Alaska (Muhs et al., 2004). Relative abundances taken from the 20.8° 2-theta peak height for quartz, 27.8° peak for plagioclase, 29.4° peak for calcite, and 31.0° peak for dolomite. (b) Plot of CaO contents (%) vs. Sr concentrations (ppm) in bulk loess (all size fractions) at Chitina compared to bulk loess in the Matanuska Valley of southern Alaska (samples of unaltered loess from localities in Muhs et al. [2004]). CaO and Sr concentrations determined by ED XRF.

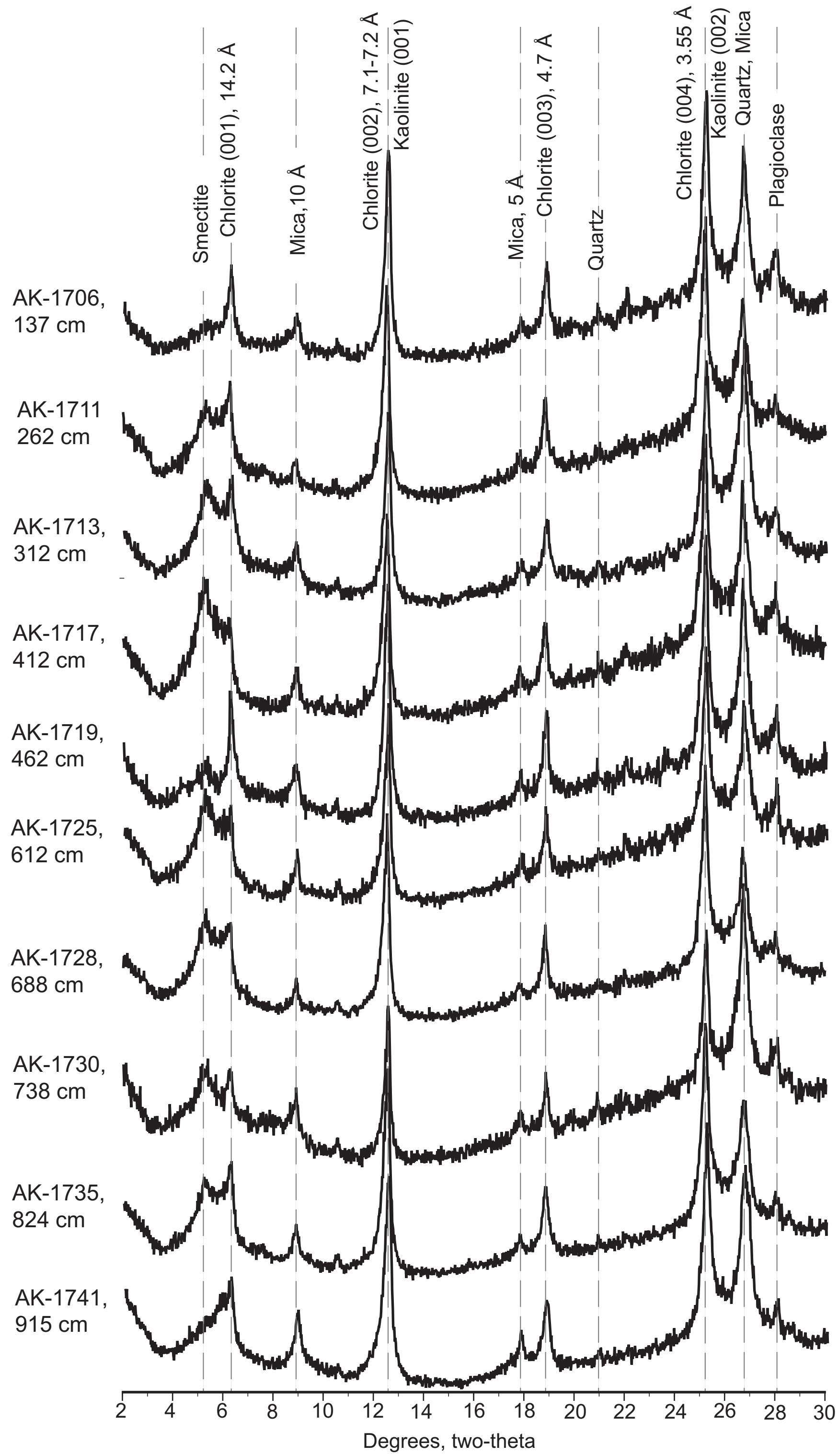

Fig. 8. X-ray diffractograms (from glycolated samples) of selected clay (<2 μm) samples from the Chitina loess section. Peak heights are roughly proportional to mineral species abundances.

7.2 Å and 3.55 Å peaks after heat treatment, it is possible some kaolinite is present.

5.4. Inferences of loess provenance from geochemistry

To compare loess at Chitina with possible source rocks, we employ plots of log [$(CaO + Na_2O)/K_2O$] vs. log (SiO_2/Al_2O_3), following Garrels and Mackenzie (1980). In arrays such as this, sandstones plot high on the log (SiO_2/Al_2O_3) axis, limestones plot high on the log [$(CaO + Na_2O)/K_2O$] axis, and shales plot low on both axes. Chitina loess falls between these three extremes, consistent with loess deposits in many regions that have an average upper crustal composition (Fig. 9). Chitina loess is not likely derived solely from rocks of the Wrangell Mountains, as the loess samples do not plot on the fields defined by bedrock types found in this mountain range (Fig. 9a). However, it is probable that the abundant Quater-

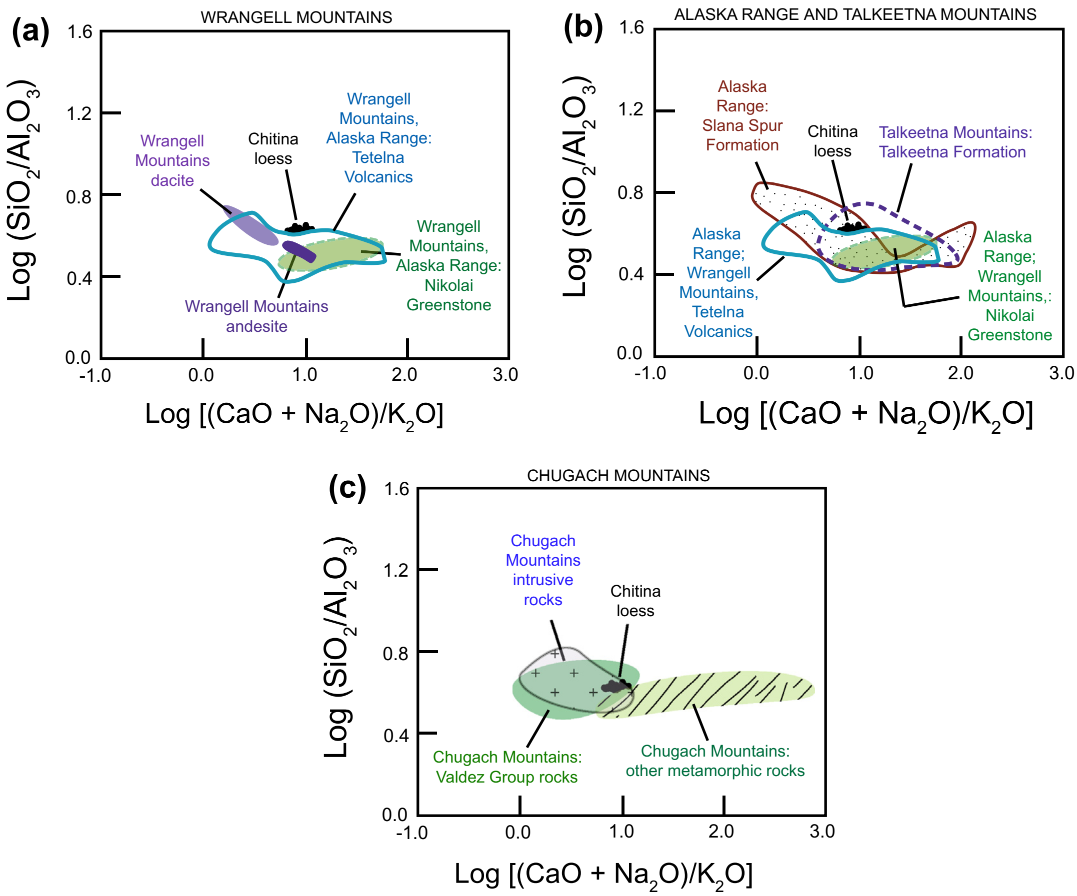

Fig. 9. Plots of Log [(CaO + Na_2O)/K_2O] vs. Log (SiO_2/Al_2O_3) in Chitina loess (<53 μm fraction; filled circles) compared to likely bedrock sources in (a) the Wrangell Mountains, (b) the Talkeetna Mountains and Alaska Range, and (c) the Chugach Mountains. Note that the Tetelna Volcanics and the Nikolai Greenstone crop out in both the Wrangell Mountains and the Alaska Range, so are shown in both (a) and (b). "Other metamorphic rocks" in (c) refers to the McHugh Complex and Liberty Creek rocks of the Chugach Terrane. Bedrock geochemical data are from Plafker et al. (1989), Barker et al. (1994), and Preece and Hart (2004).

nary and Tertiary andesites and older rocks, such as the Paleozoic Tetelna Volcanics (basalt, andesite, dacite) found in the Wrangell Mountains, are the suppliers of much of the plagioclase found in loess at Chitina. Furthermore, the Wrangell Mountains were the most likely contributors of calcite and dolomite to the loess, from the Chitistone and Nizina Limestones (Richter et al., 2006). The other mountain ranges surrounding the Copper River basin do not have abundant carbonate rocks. Chitina loess falls well within the fields defined by the Slana Spur Formation, found on the southern flanks of the eastern Alaska Range, the Talkeetna Formation, found in the eastern Talkeetna Mountains, and the Valdez Group rocks that dominate much of the Chugach Mountains (Winkler, 1992; Winkler et al., 1980) (Fig. 9b and c). The Talkeetna Formation, however, consists largely of andesitic volcaniclastic rocks (Plafker et al., 1989; Richter et al., 2006) and the Slana Spur Formation is dominated by andesite and dacite (Barker et al., 1994). These rocks could be plagioclase sources, but are not likely suppliers of minerals such as quartz, chlorite, mica, and amphibole. Derivation from glaciers that eroded rocks of the Valdez Group in the Chugach Mountains, however, explains the abundance of chlorite and amphibole in the loess at Chitina, as metasedimentary rocks of this unit include both greenschist and amphibolite facies (Winkler et al., 1980; Richter et al., 2006). The Triassic Nikolai Greenstone (Wrangell Mountains and Alaska Range) also contains chlorite (Barker et al., 1994), but its bulk chemical composition does not overlap that of the Chitina loess (Fig. 9a). We infer from the major element geochemical plots, as well as the mineralogical data, that loess at Chitina likely had contributions from rocks of the Chugach Mountains (chlorite, mica, and amphibole; possibly quartz, K-feldspar, and plagioclase) and the Wrangell Mountains (calcite and dolomite; probably plagioclase). Geochemical and mineralogical data also permit the possibility of contributions from the Alaska Range.

Trace element geochemistry can be very useful in loess provenance studies (see Muhs and Budahn, 2006, for an example from central Alaska). Plots of Sc-Th-La, La_N/Yb_N vs. Eu/Eu*, and Gd_N/Yb_N vs. Eu/Eu* provide additional discrimination of possible source rocks for loess at Chitina. Although we lack Sc-Th-La data for some of the possible source rocks in the region, these data are available for Quaternary andesites and Paleozoic volcanic rocks (Tetelna Volcanics) of the Wrangell Mountains, rocks of the Talkeetna Formation (Talkeetna Mountains), and Valdez Group rocks (Chugach Mountains). Talkeetna Formation rocks are enriched in Sc and plot very closely to the composition of average oceanic crust; in contrast, Valdez Group rocks plot closer to the composition of average upper continental crust. Both the younger and older volcanic rocks of the Wrangell Mountains plot between these extremes, consistent with their andesitic composition (Fig. 10). Chitina loess plots mostly within the field shown for the Valdez Group rocks and the uppermost parts of the Wrangell Mountains volcanic rocks, suggesting major contributions from the former and minor contributions from the latter. The rare earth element (REE) plots are consistent with the Sc-Th-La plots with regard to provenance. Although the Gd_N/Yb_N vs. Eu/Eu* plot shows considerable overlap among many of the rocks under consideration, the La_N/Yb_N vs. Eu/Eu* plot shows better discrimination between source rocks. Talkeetna Formation rocks and Nikolai Greenstone have much lower La_N/Yb_N values than Chitina loess, indicating little light REE

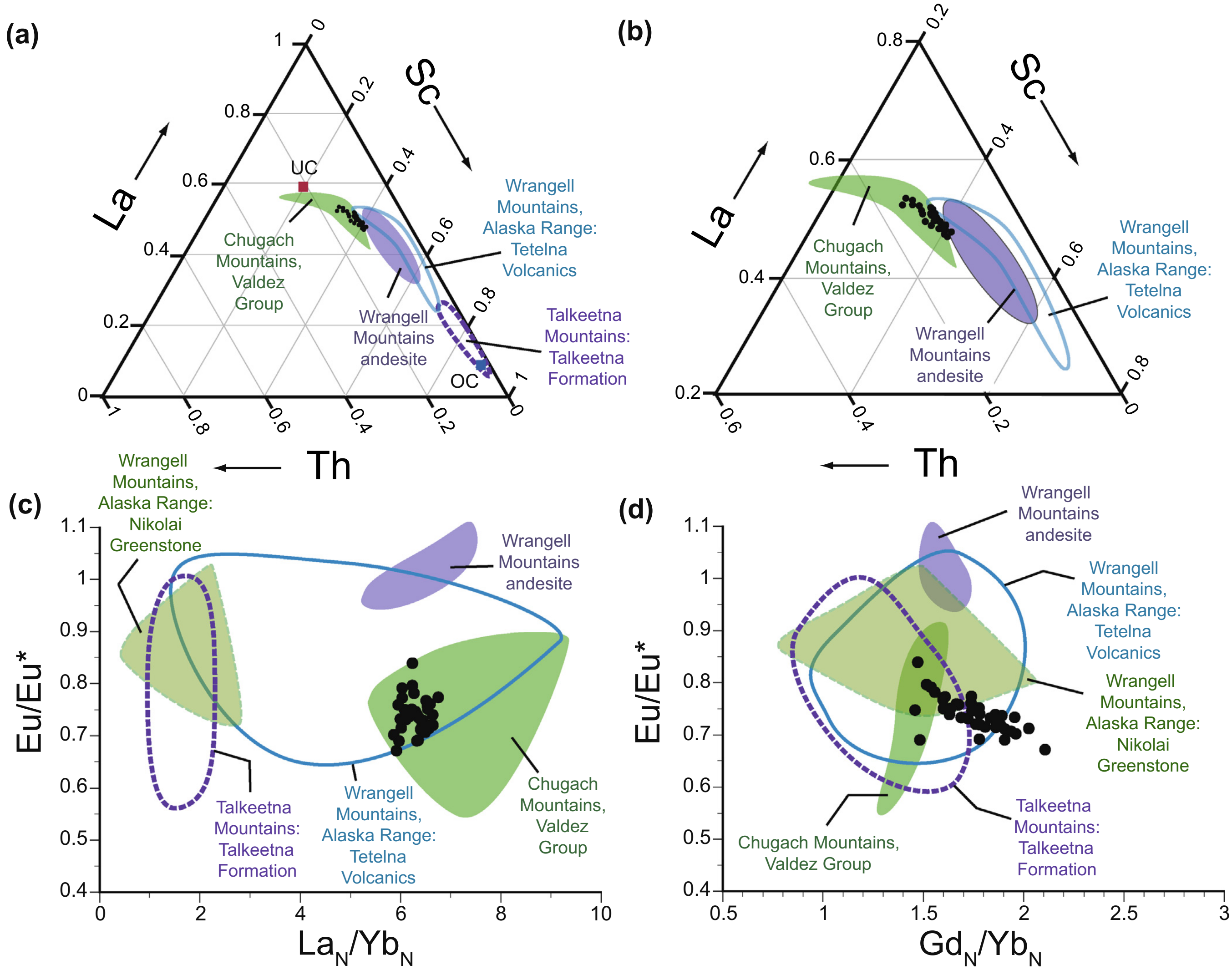

Fig. 10. (a) Sc-Th-La abundances of silt-and-clay sized (<53 μm) particles from the Chitina loess section (filled circles), along with the ranges of these values for possible bedrock sources. UC is average upper continental crust; OC is average oceanic crust (Taylor and McLennan, 1985). (b) Same as (a), but with a portion enlarged for clarity. (c) La_N/Yb_N vs. Eu/Eu* and (d) Gd_N/Yb_N vs. Eu/Eu* plots for silt-and-clay sized (<53 μm) particles from the Chitina loess section (filled circles), along with the ranges of these values for possible bedrock sources. All bedrock geochemical data from Plafker et al. (1989), Barker et al. (1994), and Preece and Hart (2004).

enrichment. Wrangell Mountains andesite has higher Eu/Eu* than loess at Chitina. The Tetelna Volcanics rocks show a very wide range of compositions on the La_N/Yb_N vs. Eu/Eu* plot, but they do overlap the range of the loess at Chitina, permitting these rocks as possible sources. Overall, rocks of the Valdez Group show the best agreement with Chitina loess on both the Sc-Th-La and La_N/Yb_N vs. Eu/Eu* plots (Figs. 10a–c).

6. Discussion

6.1. Timing of loess deposition at Chitina

Results of our studies indicate that fine-grained (silt and clay) aeolian particle entrainment, transport, and deposition have been active in the Copper River drainage basin for the entire 10,000 years of the Holocene. Worldwide, times of highest loess production are typically associated with glacial periods (see Muhs, 2013a, 2013b for reviews). The lack of a last-glacial-aged loess record at Chitina is explained by the presence of Glacial Lake Atna, which provided a sink for glaciogenic silts and clays that otherwise would have been transported as loess. Given the greater extent of glacial ice in all four mountain range surrounding the Copper River basin during the last glacial period (Fig. 3), there is little doubt that there was abundant fine particle production by glacial grinding at this time. The amount of glacial silt and clay produced during the last glacial maximum (LGM) is evident from the thickness of lacustrine silts and clays that are exposed around the Copper River drainage basin (Bennett et al., 2002). These particles were, however, deposited in Glacial Lake Atna at the LGM and were unavailable for aeolian transport. With the draining of Glacial Lake Atna at the close of the last glacial period, silt and clay entrainment by wind could proceed in the Copper River basin and, based on the stratigraphic record at Chitina, began almost immediately after lake drainage. Loess accumulation continued throughout the Holocene and up to the present. Thus, the potential for the finest-grained, aeolian portion of this sediment to reach the Gulf of Alaska has been in place for the past 10,000 years, but was probably minimal before the Holocene.

6.2. Sources of loess at Chitina

Silicate minerals comprise the majority of the particles in the Chitina loess section and include quartz, K-feldspar, plagioclase, amphibole and chlorite, with mica and carbonate minerals at most depths. Quaternary and pre-Quaternary volcanic rocks (largely andesite) and carbonate rocks of the Wrangell Mountains could have supplied much of the plagioclase, calcite and dolomite found in the loess. Tetelna Volcanics, also found in the Alaska Range, could have been an additional plagioclase contributor. The mafic volcanic rocks of both mountain ranges did not likely supply quartz, K-feldspar, amphibole, chlorite, and mica to the loess found at Chitina. However, major element and trace element (Sc-Th-La and La_N/Yb_N vs. Eu/Eu*) geochemistry are consistent with contributions from the Valdez Group rocks found in the Chugach Mountains. Valdez Group rocks include greenschist and amphibolite facies and could explain much of the quartz, chlorite, amphibole, and mica found in loess at Chitina, as all these minerals are abundant in the rocks (Plafker et al., 1992). Rocks of the Talkeetna Mountains, on the basis of trace element geochemistry, do not appear to be major contributors to loess at Chitina, but there is less glacial ice in this mountain range and only a portion of it drains to the Copper River. The main suppliers to loess at Chitina appear to be the Chugach Mountains, the Wrangell Mountains, and possibly the Alaska Range.

6.3. Importance of loess origins to iron content and comparison with other aeolian sediments

Oceanic primary production, mainly the growth of phytoplankton, is an integral part of the global carbon cycle. Falkowski et al. (1998) estimate that ~45 gigatons of organic carbon are produced each year by marine phytoplankton. As alluded to earlier, in some ocean basins, including the North Pacific Ocean, Fe is a limiting nutrient for phytoplankton growth. Delivery of fine-grained aeolian particles by the wind is one mechanism by which Fe can be delivered to the water column. Martin (1990) and Duce and Tindale (1991) propose that a major source of Fe delivery to the oceans is aeolian, long-range transport (LRT) of dust from the continents. Boyd et al. (1998), Schroth et al. (2009) and Crusius et al. (2011) have emphasized the potential importance of Copper River dust inputs as an Fe source to the Gulf of Alaska. Questions that follow from this are: (1) is the dust flux in the region significant; (2) do the loess-sized sediments from the Copper River have high Fe contents; (3) is the Fe in a form that is bioavailable; and (4) can dust from the Copper River travel be transported far enough seaward to be a significant source?

6.3.1. Mass accumulation rates

We estimate the MAR of fine-grained (<20 μm) dust over the past ~9000 years at Chitina to be 79–237 g/m^2/yr, depending on assumed bulk density values, and is most likely to be on the lower end of this range, 79–158 g/m^2/yr. Even this lower range of MARs, however, is higher than most dust flux rates worldwide, whether derived from modeling (Mahowald et al., 2006) or observational data in various geologic archives compiled in the DIRTMAP project (Kohfeld and Harrison, 2001). Contemporary dust fluxes exceeding 50 g/m^2/yr, based on modeling, are found only in the central core areas of the major desert regions of Africa, the Arabian Peninsula, central Asia, Australia, the southwestern USA, and southern South America. Late Holocene records of dust flux in deep-sea cores in the North Pacific Ocean are, with one exception, all south of ~50°N, and therefore well south of the Gulf of Alaska. Dust MARs in this region of the North Pacific Ocean are all less than 5 g/m^2/yr (Kohfeld and Harrison, 2001). The MAR calculations presented here suggest that dust fluxes farther north, in the Gulf of Alaska, may be as much as an order of magnitude higher than those south of ~50°N.

6.3.2. Iron content

Chemical analyses of loess at Chitina indicate that the fine-grained, loess-sized (<53 μm) portion of the sediment at Chitina is Fe-rich. Derivation of the loess at Chitina from rocks of three of the four mountain ranges surrounding the Copper River basin explains the high Fe content of the loess. Bulk Fe contents in these rocks (and silts and clays derived from them) are all relatively high (Fig. 11a and b). The Fe content of dust derived from the Copper River could change in the future, depending on the amount of ice retreat in each contributing mountain range.

Loess deposits from other parts of Alaska show similarities and differences to loess at Chitina. Matanuska Valley loess in southern Alaska is likely derived from rocks of the Chugach and/or Talkeetna Mountains (Muhs et al., 2004) and is similarly high in Fe (Fig. 11c). In contrast, Central Alaskan loess is derived primarily from river valleys that drain the Alaska Range and the Yukon-Tanana Upland (Muhs and Budahn, 2006), and has Fe contents somewhat lower than that of Chitina loess.

Loesses from most other parts of the world, including mid-continental North America (Illinois, Iowa, and Nebraska), South America (Argentina), and Asia (China and Siberia) show a wide range of Fe concentrations, but almost all are lower in Fe than loess at Chitina (Fig. 11c and d). An exception to this is Iceland, where loess is derived from Fe-rich basalt (Arnalds, 2010). African dust shows increases in Fe content with decreases in particle size (Fig. 11d). Based on the comparison made here, the silt + clay portion of Chitina loess is among the most Fe-rich aeolian particles reaching the world's oceans. Many researchers (e.g., Jickells et al., 2005; Mahowald et al., 2005) commonly assume that LRT dust has an average upper continental crustal Fe content of ~3.5%. The data presented here indicate that average upper continental crust values underestimate the true Fe content of dust delivered to the oceans from some regions, including much of Alaska.

6.3.3. Implications of loess mineralogy for dust-derived iron fertilization

The ability of aeolian particles to supply Fe as fertilizer to primary producers in the ocean is strongly dependent on mineralogy and Fe species. Experimental work by Journet et al. (2008) show that phyllosilicate clay minerals with ionic bonds, such as smectite and mica, yield up to two orders of magnitude more marine-water-soluble Fe compared to Fe-oxides, such as magnetite, hematite and goethite, with strong covalent bonds. Thus, dust with relatively high bulk Fe content may yield little soluble Fe to the marine environment if most of the Fe-bearing minerals are in the form of Fe-oxides. Consistent with this, Schroth et al. (2009) confirm that minerals in which Fe is in the ferrous, or Fe (II) form, yield much more Fe in leaching experiments than minerals in which Fe is in the ferric, or Fe (III) form.

Based on the silt + clay and clay-only mineralogy presented here, the main carriers of Fe in loess at Chitina are likely chlorite, amphibole, mica and smectite. Our XRD data indicate that Fe-rich chlorite is one of the most important minerals in both the silts and clays at Chitina. The majority of chlorites are trioctahedral (Moore and Reynolds, 1989), meaning that the central cation in the octahedral sheet is divalent. Thus, in Fe-rich, trioctahedral chlorites, Fe (II) is the dominant cation in the octahedral sheet and is likely bioavailable in the marine environment. Much of the Fe in amphibole minerals, also found at Chitina, is of the ferrous form, or Fe (II), and thus is also bioavailable in the marine environment. Our assessment of the bioavailability of Chitina clays and silts, based on their mineralogy, is in good agreement with Fe solubility experiments conducted by Schroth et al. (2009). These workers report that glacial flour from both the Kuskulana glacier (Wrangell Mountains) and the Matanuska glacier (Chugach and Talkeetna Mountains) yield much more soluble Fe than either Chinese loess or African dust.

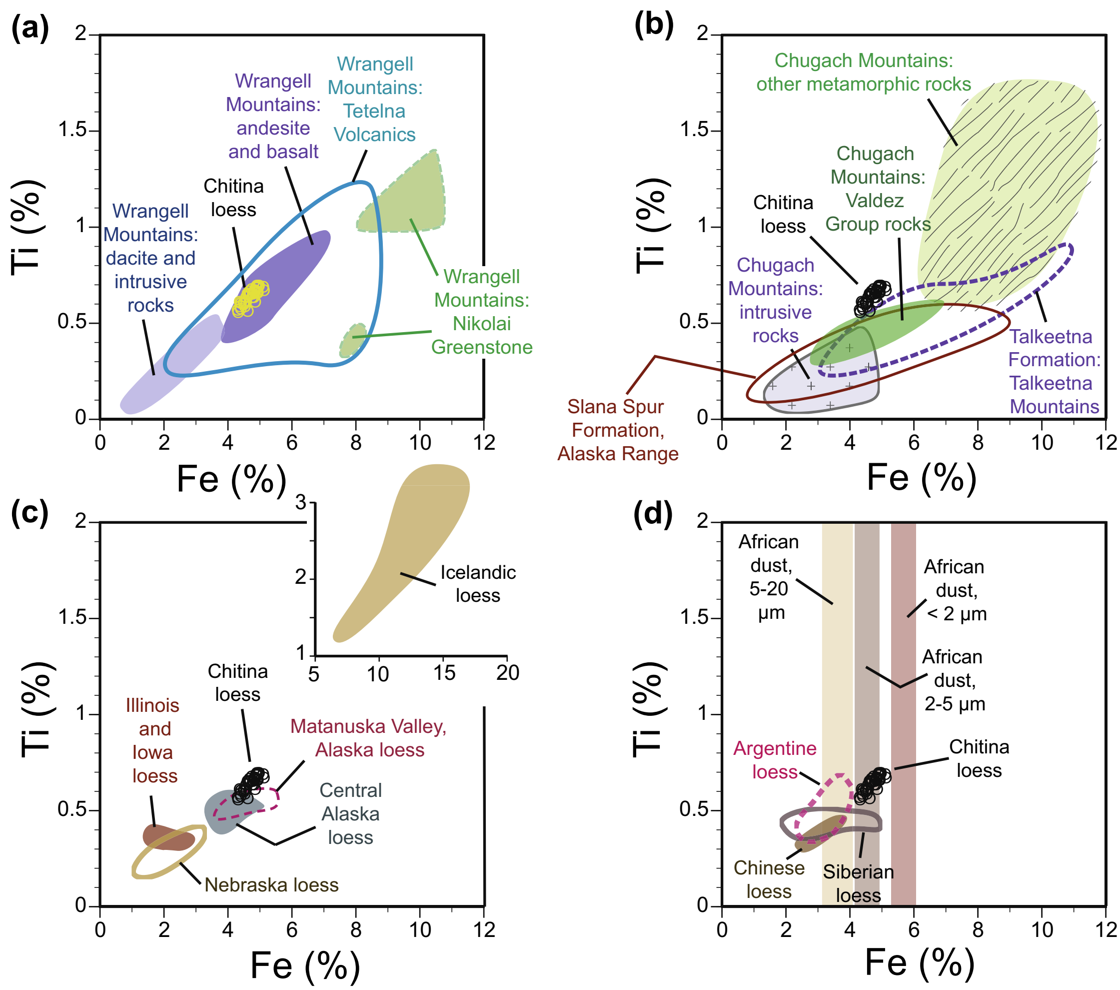

Fig. 11. Fe and Ti contents in the <53 µm (silt + clay) fraction from the Chitina loess section (open circles) compared to concentrations of these elements in possible source rocks in (a) the Wrangell Mountains, (b) the Chugach and Talkeetna Mountains and the Alaska Range, (c) bulk loesses from elsewhere in North America and Iceland (insert), and (d) loess on other continents and various size fractions of long-range-transported African dust. Bedrock geochemical data from Plafker et al. (1989), Barker et al. (1994), Sisson et al. (2003), and Preece and Hart (2004). Loess geochemical data are from Péwé and Journaux (1983), Gallet et al. (1996, 1998), Muhs and Bettis (2000), Muhs et al. (2001, 2003, 2004, 2008), Jahn et al. (2001), Schultz et al. (2004), and Jackson et al. (2005). African dust data are from Muhs et al. (2010). Because some studies report FeO and Fe_2O_3 separately, whereas other studies report total Fe as either FeO or Fe_2O_3, we converted all reported values to elemental Fe (%) and summed values if both FeO and Fe_2O_3 were reported.

6.3.4. Distance of dust transport from the Copper River basin

We recognize that much of the loess at Chitina is relatively coarse-grained aeolian silt and many particles may not be capable of LRT to the North Pacific Ocean. Thus, a question that arises is whether the loess section at Chitina is an appropriate record for LRT dust that could have been transported to the North Pacific Ocean from Alaska. Typically, LRT dust is dominated by particles with diameters <20 µm, with most having diameters <10 µm (see, for example, African dust collected on Barbados by Prospero et al. (1970)). We note that in other regions, however, coarse particles *are* capable of LRT. Betzer et al. (1988) report mineral particles >75 µm diameter that have been transported to the Pacific Ocean, more than 10,000 km from their sources in Asia. Off the west coast of Africa, Ratmeyer et al. (1999) collected particles in dust traps that are ~300–450 km from the closest possible coastal sources. They report that mean particle sizes range from ~10 to ~20 µm, but particles as large as ~55 µm were also found. Stuut et al. (2005), also working off the coast of western Africa, made shipboard dust collections, and reported modal particle sizes of 8–42 µm. However, these investigators also found a significant number of particles with diameters >100 µm.

At Chitina, above the basal sandy zones of the section, the fine silt (20–2 µm) plus clay (<2 µm) fractions range from 13% to 30% and average ~20–21%. The importance of this is that the record at Chitina shows that for the past ~10,000 years, significant amounts of fine particles with diameters <20 µm, certainly capable of LRT, have been available for aeolian transport in the Copper River basin. Further, the flux rates estimated for this fine-grained fraction are higher than those reported for other parts of the North Pacific Ocean, farther south.

A second question that arises, particularly with regard to Fe fertilization, is whether dust from southern Alaska is transported far enough to reach the open ocean, where it would be significant for phytoplankton growth. At localities near the southern coast of Alaska, Fe inputs from fluvial sources are likely to be at least as important as aeolian inputs. Well offshore, however, past the continental shelf, aeolian inputs of Fe would be much more significant for phytoplankton fertilization. Crusius et al. (2011) and Bullard (2012) present satellite imagery of the Copper River basin from several years (2005, 2006, 2009, 2010, 2011), showing that winds associated with contemporary dust storms entrain fine-grained particles and transport them at least 300 km seaward from the coast of southern Alaska, well past the

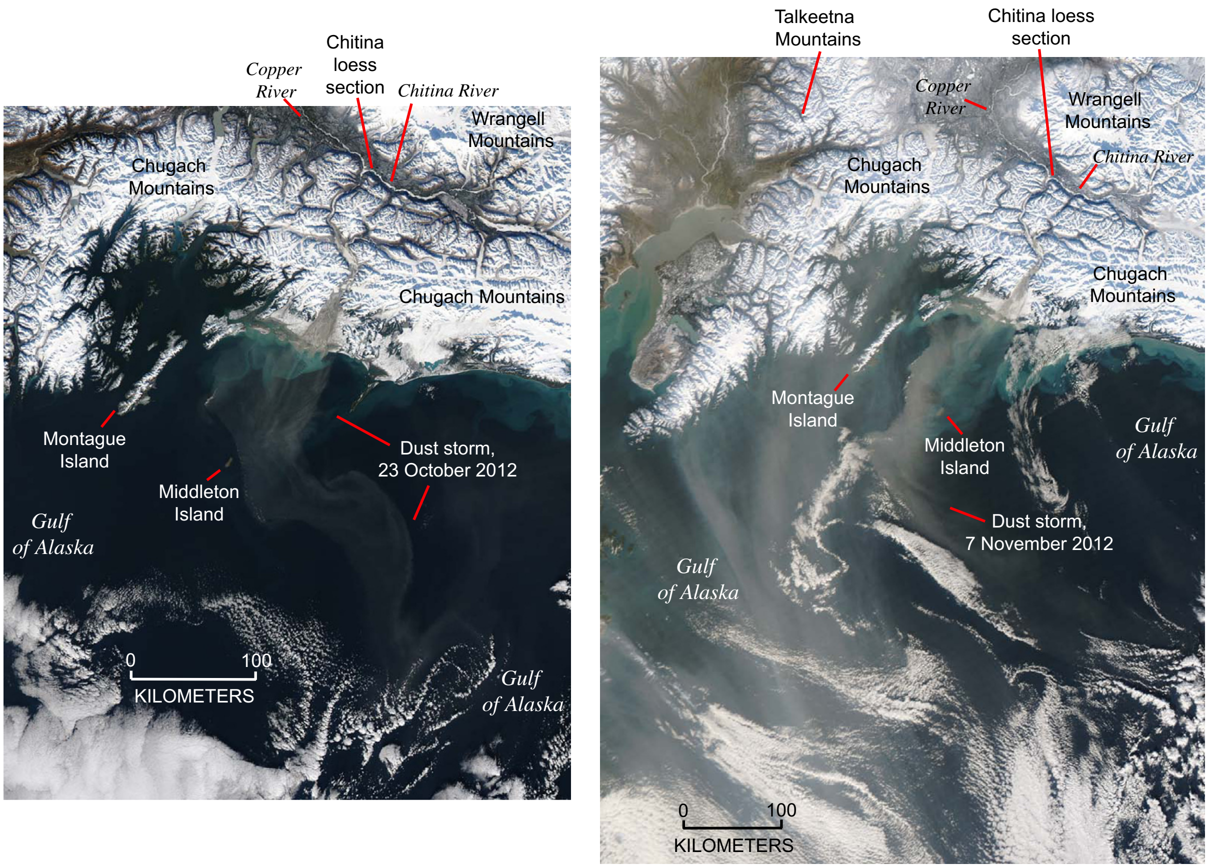

Fig. 12. Moderate Resolution Imaging Spectroradiometer (MODIS) images of southern Alaska captured by the NASA Aqua satellite on (a) 23 October 2012 and (b) 7 November 2012, showing dust transport to the Gulf of Alaska, generated by strong winds over the southern Copper River floodplain. Also shown for reference is the location of the Chitina loess section. Images courtesy of Jeff Schmaltz, LANCE MODIS Rapid Response Team at NASA GSFC.

500-m isobath and continental shelf, to the open ocean. Here we present additional satellite imagery from two very recent events, 23 October 2012 and 7 November 2012, showing similar dust storms (Fig. 12). In these images, particularly the 7 November event, dust was also transported more than 300 km from the coast of southern Alaska. This distance of transport is well out to the open ocean, as the outer edge of the continental shelf here is ~100–150 km seaward of the mouth of the Copper River. We conclude from examination of the imagery in Crusius et al. (2011) and Bullard (2012), plus the new imagery presented here, that aeolian transport of Copper River dust is capable of reaching the open North Pacific Ocean on a regular basis.

7. Summary and conclusions

(1) Loess, likely derived from the Copper River, has been accumulating at Chitina, Alaska in Wrangell-St. Elias National Park. Loess deposition occurred in a boreal forest setting, based on the presence of buried spruce stumps found throughout the section. Radiocarbon ages of these stumps and other plant materials show that dust and coarser aeolian particles have been transported from the Copper River floodplain over the past ~10,000 years, all of the present interglacial period.

(2) Based on mineralogy and geochemistry, loess at Chitina was probably derived from glacial sources in at least two mountain ranges (Wrangell Mountains and Chugach Mountains) and possibly a third (Alaska Range), indicating a complex origin for these sediments.

(3) The mineralogy of the loess at Chitina includes abundant Fe-bearing minerals. Chlorite, mica, and amphibole are found in the silt fraction, and Fe-rich chlorite, smectite, and mica dominate the clay fraction. Geochemical data are consistent with derivation of these minerals from the Chugach Mountains, where Valdez Group rocks contain both greenschist and amphibolite facies.

(4) The concentration of Fe in the silt-plus-clay fraction of the loess at Chitina is much higher than all other loess bodies in North America and higher than most loess bodies on other continents as well. The high Fe content is the result of derivation of loess from mafic volcanic rocks, metamorphosed mafic volcanic rocks, or metasedimentary rocks with mafic protoliths, all of which are high in Fe. Furthermore, this Fe is readily available to primary producers in the marine environment because of the favorable, chlorite-dominated mineralogy. Other Alaskan loess bodies are relatively high in Fe as well, and detailed clay mineralogical studies of these sediments would be a fruitful area of future research.

(5) Particle size analyses, mass accumulation rate calculations, and examination of satellite imagery show that fine-grained dust, capable of long-range transport from the Copper River, is abundant and is currently transported by wind to the open Pacific Ocean.

(6) In agreement with Bullard (2012) and Prospero et al. (2012), we conclude that contemporary glaciogenic dust at high latitudes may play an important role in the overall dust budget, particularly with respect to Fe delivery to the world's oceans. Further studies should be conducted on contemporary, high-latitude dust derived from other parts of Alaska, Canada,

Greenland, Iceland, Svalbard, and northern Russian islands in order to obtain a more quantitative assessment of the importance of this overlooked Fe source. In assessing the importance of these regions as dust sources, however, our work in southern Alaska leads us to conclude it will be necessary to investigate the source rocks for dust, the Fe content of the fine-grained aeolian particles, and their mineralogy.

Acknowledgments

This study was supported by the Climate and Land Use Change Program of the U.S. Geological Survey. We thank Tom Ager (USGS) for introducing us to the Chitina section. Jossh Beann, Jeff Pigati and Zachary Muhs Rowland (all USGS) helped in the field and Kristi Zellman, DeAnna Laurel, and Josh Freeman (all USGS) and Phil Kerr (University of Iowa) assisted in the laboratory. Thanks also go to Wrangell-St. Elias National Park (permit #WRST-2005-SCI-0020) and the Chitina Native Corporation for access to the site. Lesleigh Anderson (USGS), Tom Judkins (USGS), and two anonymous journal reviewers provided helpful comments on an earlier version of the paper.

References

Ager, T.A., 1989. History of Late Pleistocene and Holocene Vegetation in the Copper River Basin, south-central Alaska. U.S. Geological Survey Circular 1026, 89–92.
Arnalds, O., 2004. Volcanic soils of Iceland. Catena 56, 3–20.
Arnalds, O., 2010. Dust sources and deposition of aeolian materials in Iceland. Icelandic Agric. Sci. 23, 3–21.
Barker, F. et al., 1994. Some accreted volcanic rocks of Alaska and their elemental abundances. In: Plafker, G., Berg, H.C., Plafker, G. (Eds.), The Geology of Alaska, vol. v. G-1. Geological Society of America, The Geology of North America, pp. 555–587.
Bennett, M.R., Huddart, D., Thomas, G.S.P., 2002. Facies architecture within a regional glaciolacustrine basin: Copper river, Alaska. Quatern. Sci. Rev. 21, 2237–2279.
Betzer, P.R., Carder, K.L., Duce, R.A., Merrill, J.T., Tindale, N.W., Uematsu, M., Costello, D.K., Young, R.W., Feely, R.A., Breland, J.A., Bernstein, R.E., Greco, A.M., 1988. Long-range transport of giant mineral aerosol particles. Nature 336, 568–571.
Birkeland, P.W., 1999. Soils and Geomorphology. Oxford University Press, London, p. 430.
Boyd, P.W., Wong, C.S., Merrill, J., Whitney, F., Snow, J., Harrison, P.J., Gower, J., 1998. Atmospheric iron supply and enhanced vertical carbon flux in the NE subarctic Pacific: Is there a connection? Global Biogeochem. Cycles 12, 429–441.
Bronk Ramsey, C., 2009. Bayesian analysis of radiocarbon dates. Radiocarbon 51, 337–360.
Brown, J., Ferrians, O.J., Jr., Heginbottom, J.A., Melnikov, E.S., 1997. Circum-Arctic map of permafrost and ground-ice conditions. U.S. Geological Survey Map CP-45, scale 1:10,000,000.
Bullard, J.E., 2012. Contemporary glacigenic inputs to the dust cycle. Earth Surf. Proc. Land. 38, 71–89.
Budahn, J.R., Wandless, G.A., 2002. Instrumental Neutron Activation by Long Count. U.S. Geological Survey Open-File Report OF 02-0223, X1–X13.
Crusius, J., Schroth, A.W., Gassó, S., Moy, C.M., Levy, R.C., Gatica, M., 2011. Glacial flour dust storms into the Gulf of Alaska: hydrologic and meteorological controls and their importance as a source of bioavailable iron. Geophys. Res. Lett. 38. http://dx.doi.org/10.1029/2010GL046573.
Duce, R.A., Tindale, N.W., 1991. Atmospheric transport of iron and its deposition in the ocean. Limnol. Oceanogr. 36, 1715–1726.
Engleman, E.E., Jackson, L.L., Norton, D.R., 1985. Determination of carbonate carbon in geological materials by coulometric titration. Chem. Geol. 53, 125–128.
EPICA Community Members, 2004. Eight glacial cycles from an Antarctic ice core. Nature 429, 623–628.
Falkowski, P.G., Barber, R.T., Smetacek, V., 1998. Biogeochemical controls and feedbacks on ocean primary production. Science 281, 200–206.
Ferrians Jr., O.J., 1989. Glacial Lake Atna Copper River Basin, Alaska. U.S. Geological Survey Circular 1026, pp. 85–88.
Gallet, S., Jahn, B., Torii, M., 1996. Geochemical characterization of the Luochuan loess-paleosol sequence, China, and paleoclimatic implications. Chem. Geol. 133, 67–88.
Gallet, S., Jahn, B., Van Vliet-Lanoe, B., Dia, A., Rossello, E.A., 1998. Loess geochemistry and its implications for particle origin and composition of the upper continental crust. Earth Planet. Sci. Lett. 156, 157–172.
Garrels, R.M., Mackenzie, F.T., 1980. Evolution of Sedimentary Rocks. W.W. Norton & Company, Inc., New York, p. 397.
Goudie, A.S., Middleton, N.J., 2006. Desert Dust in the Global System. Springer, Heidelberg, p. 287.
Hopkins, D.M., 1963. Geology of the Imuruk Lake area, Seward Peninsula, Alaska. U.S. Geological Survey Bulletin1141-C.
Jackson, M.G., Oskarsson, N., Trønnes, R.G., McManus, J.F., Oppo, D.W., Grönvold, K., Hart, S.R., Sachs, J.P., 2005. Holocene loess deposition in Iceland: evidence for millennial-scale atmosphere-ocean coupling in the North Atlantic. Geology 33, 509–512.
Jahn, B., Gallet, S., Han, J., 2001. Geochemistry of the Xining, Xifeng and Jixian sections, Loess Plateau of China: eolian dust provenance and paleosol evolution during the last 140 ka. Chem. Geol. 178, 71–94.
Jickells, T.D., An, Z.S., Andersen, K.K., Baker, A.R., Bergametti, G., Brooks, N., Cao, J.J., Boyd, P.W., Duce, R.A., Hunter, K.A., Kawahata, H., Kubilay, N., LaRoche, J., Liss, P.S., Mahowald, N., Prospero, J.M., Ridgwell, A.J., Tegen, I., Torres, R., 2005. Global iron connections between desert dust, ocean biogeochemistry, and climate. Science 308, 67–71.
Journet, E., Desboeufs, K.V., Caquineau, S., Colin, J.-L., 2008. Mineralogy as a critical factor of dust iron solubility. Geophys. Res. Lett. 35, L07805. http://dx.doi.org/10.1029/2007/GL031589.
Karlstrom, T.N.V., Coulter, H.W., Fernald, A.T., Williams, J.R., Hopkins, D.M., Péwé, T.L., Drewes, H., Muller, E.H., Condon, W.H., 1964. Surficial geology of Alaska. U.S. Geological Survey Miscellaneous Geologic Investigations Map I-357, scale 1:1,584,000.
Kohfeld, K.E., Harrison, S.P., 2001. DIRTMAP: the geological record of dust. Earth-Sci. Rev. 54, 81–114.
Kohfeld, K.E., Tegen, I., 2007. Record of mineral aerosols and their role in the Earth system. In: Holland, H.D., Turekian, K.K. (Eds.), Treatise on Geochemistry, Elsevier, vol. 14, p. 26. Available from: <http://www.sciencedirect.com/science/referenceworks/9780080437514>.
Lam, P.J., Bishop, J.K.B., 2008. The continental margin is a key source of iron to the HNLC North Pacific Ocean. Geophys. Res. Lett. 35, L07608. http://dx.doi.org/10.1029/2008GL033294.
Maher, B.A., Prospero, J.M., Mackie, D., Gaiero, D., Hesse, P., Balkanski, Y., 2010. Global connections between aeolian dust, climate and ocean biogeochemistry at the present day and at the last glacial maximum. Earth-Sci. Rev. 99, 61–97.
Mahowald, N.M., Baker, A.R., Bergametti, G., Brooks, N., Duce, R.A., Jickells, T.D., Kubilay, N., Prospero, J.M., Tegen, I., 2005. Atmospheric global dust cycle and iron inputs to the ocean. Global Biogeochem. Cycles 19. http://dx.doi.org/10.1029/2004GB002402 (GB4025).
Mahowald, N.M., Muhs, D.R., Levis, S., Rasch, P.J., Yoshioka, M., Zender, C.S., Luo, C., 2006. Change in atmospheric mineral aerosols in response to climate: last glacial period, preindustrial, modern, and doubled carbon dioxide climates. J. Geophys. Res. 111. http://dx.doi.org/10.1029/2005JD006653.
Martin, J.H., 1990. Glacial-interglacial CO_2 change: the iron hypothesis. Paleoceanography 5, 1–13.
McGeehin, J., Burr, G.S., Jull, A.J.T., Reines, D., Gosse, J., Davis, P.T., Muhs, D., Southon, J.R., 2001. Stepped-combustion ^{14}C dating of sediment: a comparison with established techniques. Radiocarbon 43, 255–261.
Moore, D.M., Reynolds Jr., R.C., 1989. X-ray Diffraction and the Identification and Analysis of Clay Minerals. Oxford University Press, Oxford, p. 332.
Muhs, D.R., 2013a. Geologic records of dust in the Quaternary. Aeolian Res. 9, 3–48.
Muhs, D.R., 2013b. Loess and its geomorphic, stratigraphic, and paleoclimatic significance in the Quaternary. In: Shroder, John.F. (Ed.), Treatise on Geomorphology, Vol. 11. Academic Press, San Diego, pp. 149–183.
Muhs, D.R., Bettis III, E.A., 2000. Geochemical variations in Peoria loess of western Iowa indicate paleowinds of midcontinental North America during last glaciation. Quatern. Res. 53, 49–61.
Muhs, D.R., Budahn, J., 2006. Geochemical evidence for the origin of late Quaternary loess in central Alaska. Can. J. Earth Sci. 43, 323–337.
Muhs, D.R., Bettis III, E.A., Been, J., McGeehin, J., 2001. Impact of climate and parent material on chemical weathering in loess-derived soils of the Mississippi River Valley. Soil Sci. Soc. Am. J. 65, 1761–1777.
Muhs, D.R., McGeehin, J.P., Beann, J., Fisher, E., 2004. Holocene loess deposition and soil formation as competing processes, Matanuska Valley, southern Alaska. Quatern. Res. 61, 265–276.
Muhs, D.R., Budahn, J., Skipp, G., Prospero, J.M., Patterson, D., Bettis III, E.A., 2010. Mineralogical and geochemical evidence for Sahara and Sahel dust additions to Quaternary soils on Lanzarote, eastern Canary Islands, Spain. Terra Nova 22, 399–410.
Muhs, D.R., Ager, T.A., Bettis III, E.A., McGeehin, J., Been, J.M., Begét, J.E., Pavich, M.J., Stafford Jr., T.W., Stevens, D.S.P., 2003. Stratigraphy and paleoclimatic significance of late Quaternary loess-paleosol sequences of the Last Interglacial-Glacial cycle in central Alaska. Quatern. Sci. Rev. 22, 1947–1986.
Muhs, D.R., Bettis III, E.A., Aleinikoff, J., McGeehin, J.P., Beann, J., Skipp, G., Marshall, B.D., Roberts, H.M., Johnson, W.C., Benton, R., 2008. Origin and paleoclimatic significance of late Quaternary loess in Nebraska: evidence from stratigraphy, chronology, sedimentology, and geochemistry. Geol. Soc. Am. Bull. 120, 1378–1407.
Nichols, D.R., 1989. Pleistocene glacial events southeastern Copper River basin, Alaska. US Geological Survey Circular 1026, pp. 78–80.
Péwé, T.L., 1975. Quaternary Geology of Alaska. U.S. Geological Survey Professional Paper 835, p. 145.
Péwé, T.L., 1983. Origin and Character of Loesslike Silt in Unglaciated South-central Yakutia, Siberia. U.S.S.R. U.S. Geological Survey Professional Paper 1262, p. 46.
Plafker, G., Nokleberg, W.J., Lull, J.S., 1989. Bedrock geology and tectonic evolution of the Wrangellia, Peninsular, and Chugach terranes along the Trans-Alaska Crustal Transect in the Chugach Mountains and southern Copper River basin, Alaska. J. Geophys. Res. 94, 4255–4295.

Plafker, G., Lull, J.S., Nokleberg, W.J., Pessel, G.H., Wallace, W.K., Winkler, G.R., 1992. Geologic map of the Valdez A-4, B-3, B-4, C-3, C-4, and D-4 quadrangles, northern Chugach Mountains and southern Copper River Basin, Alaska. U.S. Geological Survey, Miscellaneous Investigations Series Map I-2164, scale 1:125000.

Preece, S.J., Hart, W.K., 2004. Geochemical variations in the <5 Ma Wrangell Volcanic Field, Alaska: implications for the magmatic and tectonic development of a complex arc system. Tectonophysics 392, 165–191.

Prospero, J.M., Bullard, J.E., Hodgkins, R., 2012. High-latitude dust over the north Atlantic: inputs from Icelandic proglacial dust storms. Science 335, 1078–1082.

Prospero, J.M., Bonatti, E., Schubert, C., Carlson, T.N., 1970. Dust in the Caribbean atmosphere traced to an African dust storm. Earth Planet. Sci. Lett. 9, 287–293.

Prospero, J.M., Ginoux, P., Torres, O., Nicholson, S.E., Gill, T.E., 2002. Environmental characterization of global sources of atmospheric soil dust identified with the Nimbus 7 Total Ozone Mapping Spectrometer (TOMS) absorbing aerosol product. Rev. Geophys. 40, 1002. http://dx.doi.org/10.1029/2000RG000095.

Ratmeyer, V., Fischer, G., Wefer, G., 1999. Lithogenic particle fluxes and grain size distributions in the deep ocean off northwest Africa: implications for seasonal changes of aeolian dust input and downward transport. Deep Sea Res. I 46, 1289–1337.

Rea, D.K., 1994. The paleoclimatic record provided by eolian deposition in the deep sea: the geologic history of wind. Rev. Geophys. 32, 159–195.

Rea, D.K., 2007. Eolian records, deep-sea sediments. In: Elias, S. (Ed.), The Encyclopedia of Quaternary Sciences. Elsevier, Amsterdam, pp. 643–649.

Reimer, P.J., Baillie, M.G.L., Bard, E., Bayliss, A., Beck, J.W., Blackwell, P.G., Bronk Ramsey, C., Buck, C.E., Burr, G.S., Edwards, R.L., Friedrich, M., Grootes, P.M., Guilderson, T.P., Hajdas, I., Heaton, T.J., Hogg, A.G., Hughen, K.A., Kaiser, K.F., Kromer, B., McCormac, F.G., Manning, S.W., Reimer, R.W., Richards, D.A., Southon, J.R., Talamo, S., Turney, C.S.M., van der Plicht, J., Weyhenmeyer, C.E., 2009. IntCal09 and Marine09 radiocarbon age calibration curves, 0–50,000 years cal BP. Radiocarbon 51, 1111–1150.

Richter, D.H., Preller, C.C., Labay, K.A., Shew, N.B., 2006. Geologic map of the Wrangell-St. Elias National Park and Preserve, Alaska. U.S. Geological Survey Scientific Investigations Map 2877, scale 1:350,000.

Rubin, M., Alexander, C., 1960. U.S. Geological Survey radiocarbon dates V. Am. J. Sci. Radiocarbon Suppl. 2, 129–185.

Ruth, U., Bigler, M., Röthlisberger, R., Siggaard-Andersen, M.-L., Kipfstuhl, S., Goto-Azuma, K., Hansson, M.E., Johnsen, S.J., Lu, H., Steffensen, J.P., 2007. Ice core evidence for a very tight link between North Atlantic and East Asian glacial climate. Geophys. Res. Lett. 34. http://dx.doi.org/10.1029/2006GL027876.

Sainsbury, C.L., 1972. Geologic Map of the Teller Quadrangle, Western Seward Peninsula, Alaska. U.S. Geological Survey Miscellaneous Geologic Investigations Map I-685, scale 1:250,000.

Schroth, A.W., Crusius, J., Sholkovitz, E.R., Bostick, B.C., 2009. Iron solubility driven by speciation in dust sources to the ocean. Nat. Geosci. 2, 337–340.

Schultz, P.H., Zárate, M., Hames, B., Koeberl, C., Bunch, T., Storzer, D., Renne, P., Wittke, J., 2004. The Quaternary impact record from the Pampas, Argentina. Earth Planet. Sci. Lett. 219, 221–238.

Shao, Y., Wyrwoll, K.-H., Chappell, A., Huang, J., Lin, Z., McTainsh, G.H., Mikami, M., Tanaka, T.Y., Wang, X., Yoon, S., 2011. Dust cycle: an emerging theme in Earth system science. Aeolian Res. 2, 181–204.

Sisson, V.V., Poole, A.R., Harris, N.R., Burner, H.C., Pavlis, T.L., Copeland, P., Donelick, R.A., McLelland, W.C., 2003. Geochemical and geochronologic constraints for genesis of a tonalite-trondhjemite suite and associated mafic intrusive rocks in the eastern Chugach Mountains, Alaska: a record of ridge-transform subduction. Geol. Soc. Am. Spec. Pap. 371, 293–326.

Stuut, J.-B., Zabel, M., Ratmeyer, V., Helmke, P., Schefuß, E., Lavik, G., Schneider, R., 2005. Provenance of present-day eolian dust collected off NW Africa. J. Geophys. Res. 110, D04202. http://dx.doi.org/10.1029/2004JD005161.

Tarr, R.S., Martin, L., 1913. Glacial deposits of the continental type in Alaska. Journal of Geology 21, 289–300.

Taylor, S.R., McLennan, S.M., 1985. The Continental Crust: Its Composition and Evolution. Blackwell Scientific Publications, Oxford, p. 312.

Tegen, I., 2003. Modeling the mineral dust aerosol cycle in the climate system. Quatern. Sci. Rev. 22, 1821–1834.

Tinner, W., Hu, F.S., Beer, R., Kaltenrieder, P., Scheurer, B., Krähenbühl, U., 2006. Postglacial vegetational and fire history: pollen, plant macrofossil and charcoal records from two Alaskan lakes. Veg. History Archaeobot. 15, 279–293.

Wiedmer, M., Montgomery, D.R., Gillespie, A.R., Greenberg, H., 2010. Late Quaternary megafloods from Glacial Lake Atna, Southcentral Alaska, U.S.A.. Quatern. Res. 73, 413–424.

Williams, J.R., 1989. A working glacial chronology for the western Copper River basin, Alaska. U.S. Geological Survey Circular 1026, pp. 81–84.

Winkler, G.R., 1992. Geologic map and summary geochronology of the Anchorage 1° × 3° quadrangle, southern Alaska. U.S. Geological Survey Miscellaneous Investigations Series Map I-2283, scale 1:250,000.

Winkler, G.R., Miller, R.J., Grantz, A., MacKevett, E.M., Jr., Silberman, M.L., Plafker, G., Case, J.E., 1980. Geologic map of the Valdez 1° x 3° quadrangle, southern Alaska. U.S. Geological Survey Open-File Report 80–892-A, scale 1:250,000.

Williams, J.R., 2000. A Geologic Guide to Wrangell-St. Elias National Park and Preserve, Alaska. U.S. Geological Survey Professional Paper 1616, p. 166.